



## MODELLING OSCILLATIONS AND WAVES OF CYTOSOLIC CALCIUM

GENEVIEVE DUPONT and ALBERT GOLDBETER

Faculté des Sciences, Université Libre de Bruxelles, Campus Plaine CP231, Boulevard  
du Triomphe, B-1050 Brussels, Belgium

Key words and phrases: calcium, oscillations, waves, inositol 1,4,5-trisphosphate,  
calcium-induced calcium release, calcium spirals

### 1. INTRODUCTION

In most cell types, calcium signals are highly organized in time and space [1,2]. After stimulation by an extracellular agonist activating the phosphoinositide signalling pathway, intracellular organelles such as the endo- or sarcoplasmic reticulum release calcium into the cytoplasm. Because of the regenerative properties of the inositol 1,4,5-trisphosphate (InsP<sub>3</sub>) and ryanodine receptors that regulate this release, there is a periodic exchange of calcium between the internal stores and the cytosol. Calcium oscillations are so widespread that they can be regarded as one of the most significant findings of the last decade in the field of intracellular organization [3]. Depending on the cell type and the extracellular agonist, calcium oscillations vary in period (from a few seconds to tens of minutes), shape (transient spikes or sinusoidal oscillations), and sensitivity to different drugs. For a given cell, the frequency of spiking increases with the level of extracellular calcium, while the amplitude remains roughly constant. Such frequency-encoded signals may be used to convey information into the cell interior [4,5].

Calcium oscillations are moreover organized spatially at the subcellular level. Thus, in stimulated cells, the successive calcium spikes do not occur synchronously throughout the cytoplasm but originate from a specific locus. This spatial propagation of an initially localized calcium increase has long been observed to play a primary role in a variety of eggs after fertilization [6]. The shape and propagation velocity of calcium waves also seem to differ from one cell type to another. In some cell types, such as cardiac cells [7], waves propagate as sharp bands with velocities and frequencies that are high enough to allow for the simultaneous propagation of distinct fronts in a given individual cell. The latter type of wave has been called type 1 [8]. In contrast, waves of type 2, also referred to as "tides" [9], have been defined as ones in which the level of calcium progressively rises along the entire cell before returning to the basal level in a quasi-homogeneous manner. This behaviour has been reported for eggs [6], hepatocytes [10], and endothelial cells [11].

In *Xenopus* oocytes [12] and in rat cardiac myocytes [13,14], propagation of intracellular spiral calcium waves has also been observed. In the huge *Xenopus* oocyte (1mm diameter), spiral waves seem to be created by the interference between multiple circular waves. In contrast, in myocytes, the calcium front, which is initially planar, transforms into a spiral near a nucleus. The front then spins around the latter obstacle at a frequency of about 1 Hz.

From a physico-chemical point of view, intracellular calcium signalling behaves as an auto-organized phenomenon [3,15]. Through  $\text{InsP}_3$  synthesis, the extracellular stimulus transforms the cytosol into an excitable matrix, able to amplify any local perturbation, or to generate sustained oscillations when the cellular environment is slightly modified. A first class of models for calcium oscillations rely on an oscillating level of  $\text{InsP}_3$  [16,17]. However, as calcium oscillations can be induced by nonmetabolizable analogues of  $\text{InsP}_3$ , it is generally thought that an additional regulation must play a key role in their occurrence. A possible regulation providing a positive feedback responsible for the oscillatory behaviour would be that the calcium releasing activity of the channels embedded in the membranes of the intracellular stores increases with the level of cytosolic calcium. This regulation, which had long been demonstrated in cardiac cells [18] is known as calcium-induced calcium release (CICR). The CICR mechanism is at the core of initial, phenomenological models for calcium oscillations [19,20,21]. Experimental studies have later demonstrated that the  $\text{InsP}_3$  receptor is indeed activated by cytosolic calcium [22,23]. Molecular models based on a detailed description of the dynamics of the  $\text{InsP}_3$  receptor were then developed [24,25]. The positive feedback exerted by cytosolic calcium on its own increase however remains the key element providing sustained oscillations. Along that line, the phenomenological and simple two-variable model [20,21] used in the present study keeps being a useful and appropriate tool to study the dynamics of intracellular calcium signalling.

## 2. TWO-VARIABLE MODEL BASED ON CALCIUM-INDUCED CALCIUM RELEASE

In building models for calcium oscillations based on CICR, the question arises as to the molecular entity where activation of calcium release by cytosolic calcium occurs. In many cells such as *Xenopus* oocytes [26,27] or Purkinje cells [22,23], calcium and  $\text{InsP}_3$  behave as co-agonists for calcium release. On the other hand, the existence of two types of calcium pools, one sensitive to  $\text{InsP}_3$  (possessing  $\text{InsP}_3$  receptors) and one sensitive to calcium (possessing caffeine/ryanodine receptors) has been demonstrated in other cells such as adrenal chromaffin cells [28], pituitary cells [29], Purkinje neurons [30], acinar cell [31], smooth muscle cells [32] and sea urchin eggs [33]. The control of calcium-sensitive,  $\text{InsP}_3$ -insensitive pools could be more complex than what has been considered so far, as it has been demonstrated that the calcium channel function of the ryanodine receptor can be modulated by cyclic ADP-ribose [33,34,35].

In the first model based on CICR, we initially considered the existence of two distinct types of pools (see Fig. 1A). A detailed analysis of that model has been presented elsewhere [20,21,36]. Here, we simply recall the kinetic equa-

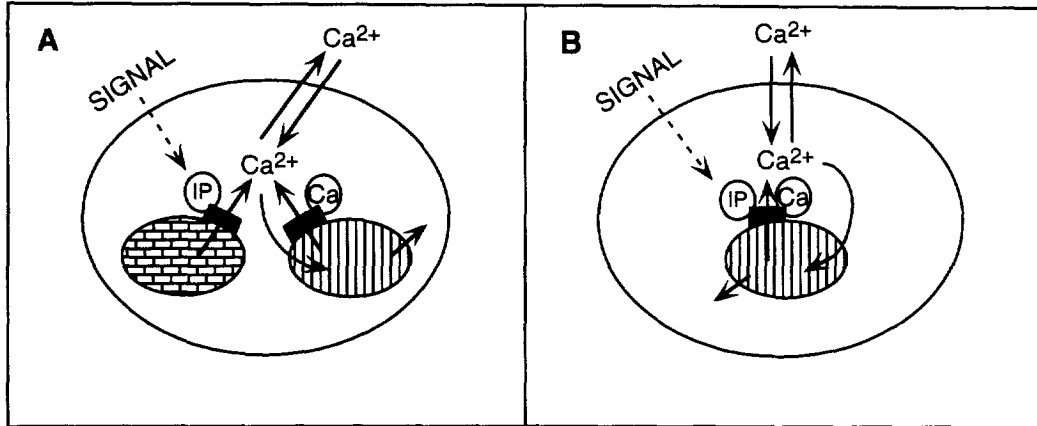


Fig.1. Schematic representation of the two-pool (A) and one-pool (B) models for calcium oscillations based on CICR. In both cases the level of InsP<sub>3</sub> (IP), which increases with the level of external stimulation, is assumed to remain constant. Cytosolic calcium activates the release of calcium from an InsP<sub>3</sub>-insensitive, calcium-sensitive store (A) or from a calcium- and InsP<sub>3</sub>-sensitive store (B).

tions of the model together with the definition of the parameters. As the InsP<sub>3</sub> level is assumed to remain constant as long as external stimulation is maintained, the model contains only two variables, namely cytosolic (Z) and intravesicular (Y) calcium. When taking into account the two-dimensional diffusion of cytosolic calcium within a planar section through the cell, the time evolution of cytosolic and intravesicular calcium is given by the following differential equations:

$$\frac{dZ}{dt} = V_{in} - V_2 + V_3 + k_f Y - kZ + D_Z \left( \frac{\partial^2 Z}{\partial x^2} + \frac{\partial^2 Z}{\partial y^2} \right) \quad (1)$$

$$\frac{dY}{dt} = V_2 - V_3 - k_f Y$$

with:

$$V_{in} = v_0 + v_1 \beta \quad (2)$$

$$V_2 = V_{M2} \frac{Z^n}{K_2^n + Z^n} \quad (3)$$

$$V_3 = V_{M3} \frac{Y^m}{K_R^m + Y^m} \frac{Z^p}{K_A^p + Z^p} \quad (4a)$$

In these equations,  $V_{in}$  represents the total, constant entry of calcium into the cytosol; it includes the background influx  $v_0$  from the extracellular medium and the InsP<sub>3</sub>-stimulated calcium influx  $v_1\beta$  from the InsP<sub>3</sub>-sensitive store ( $\beta$  is the degree of saturation of the InsP<sub>3</sub> receptor);  $V_2$  and  $V_3$  are, respectively, the rates of pumping into and release from the calcium-sensitive store with  $V_{M2}$  and  $V_{M3}$  denoting the maximum rates of these processes;  $K_2, K_R$  and  $K_A$  are the threshold constants for pumping, release and activation while  $n, m$  and  $p$  are the Hill coefficients characterizing these processes;  $k_f Y$  and  $kZ$  refer to the passive efflux from the calcium-sensitive store and from the cytosol;  $DZ$  is the diffusion coefficient for cytosolic calcium. Diffusion is considered in two spatial dimensions, denoted  $x$  and  $y$ .

#### *One-pool version of the model based on InsP<sub>3</sub>-sensitive CICR*

When only one type of calcium pool is considered, with InsP<sub>3</sub> and calcium acting as co-agonists for calcium release (Fig. 1B), the model based on CICR defined by eqs. (1) can still account for the existence and for the main properties of calcium oscillations [37]. The kinetic equations describing the evolution of cytosolic calcium and of calcium in the store sensitive to InsP<sub>3</sub> and calcium are then only slightly modified. To account for the fact that the same receptor/channel is activated by both InsP<sub>3</sub> and calcium, the term  $V_3$  which now represents the calcium release from the unique calcium- and InsP<sub>3</sub>-sensitive store is given by:

$$V_3 = \beta V_{M3} \frac{Y^m}{K_R^m + Y^m} \frac{Z^p}{K_A^p + Z^p} \quad (4b)$$

where  $\beta$  represents the degree of saturation by InsP<sub>3</sub> of this 'bi-activated' receptor and  $V_{M3}$  the maximum rate of release. The constant calcium influx into the cytosol is still given by eq. (2) but the meaning of  $v_1\beta$  has changed: it now represents a stimulus-activated calcium influx from the extracellular medium into the cytosol. The consideration of such a regulated calcium entry, which is supported by recent experimental data [38,39,40], allows one to keep the property that the mean calcium level increases with the degree of stimulation. With regard to oscillations the two forms of the CICR model only differ by the amplitude of the first spike and by its latency, i.e. the time that separates it from the onset of stimulation [41].

### 3. TEMPORAL OSCILLATIONS

When global intracellular calcium changes in response to external stimulation are measured, the variations in the level of this second messenger represent

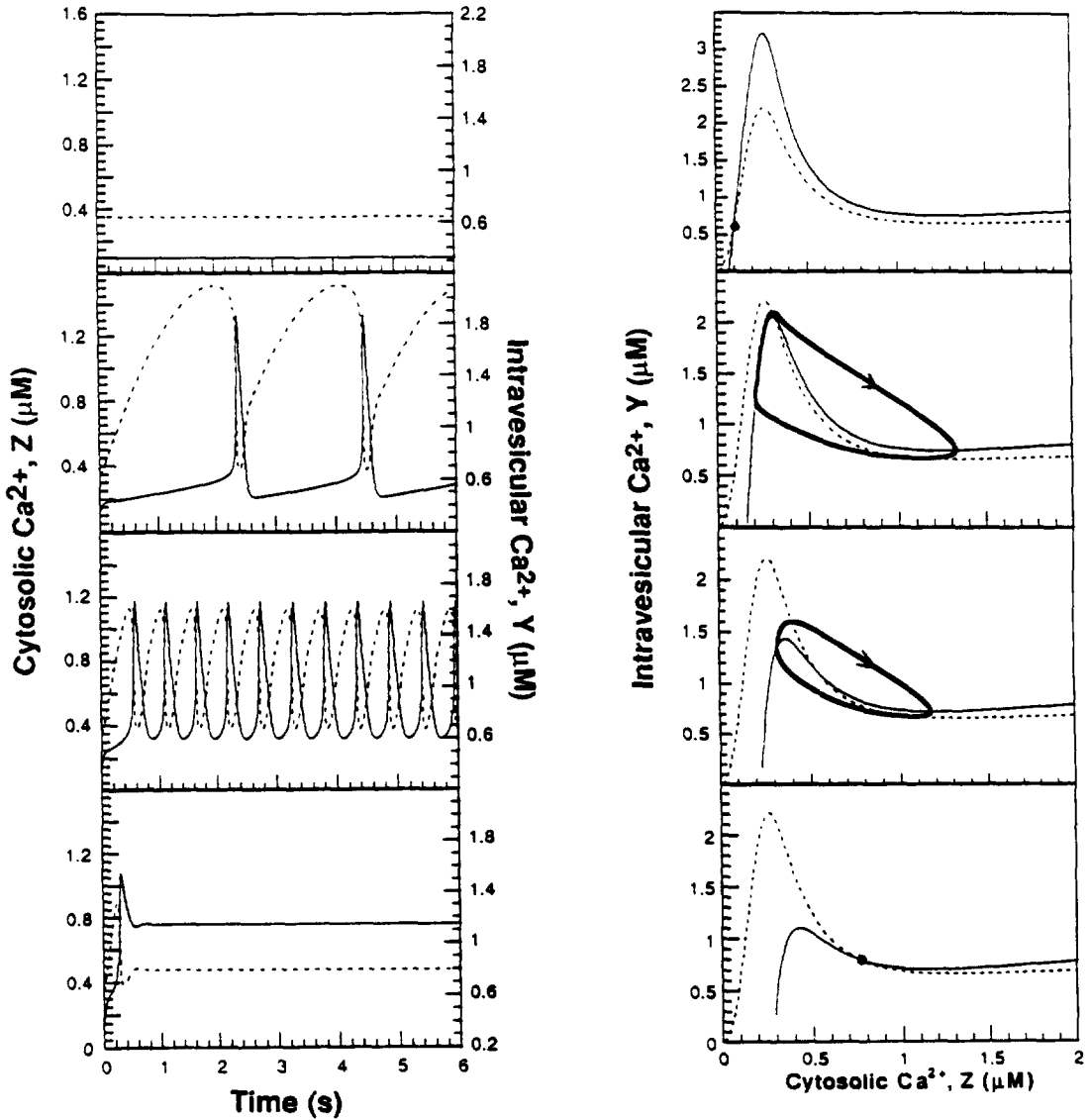


Fig.2. Behaviour of the spatially homogeneous two-pool model based on CICR (eqs. (1)-(4a) without diffusion of cytosolic calcium) for increasing levels of stimulation ( $\beta = 0, 30, 60$  and  $90\%$  from top to bottom). LEFT: evolution of cytosolic (plain line) and intravesicular (dashed line) calcium as a function of time. In all panels, the initial condition corresponds to the stationary state in the absence of stimulation ( $\beta = 0$ ). RIGHT: the stationary state or the limit cycle (bold line) is shown together with the null-clines  $dZ/dt = 0$  (plain line) and  $dY/dt = 0$  (dashed line). Results have been obtained by numerical integration of eqs. (1)-(4a) with the following parameter values:  $v_0 = 1 \mu\text{M/s}$ ,  $v_1 = 7.3 \mu\text{M/s}$ ,  $K_R = 2 \mu\text{M}$ ,  $V_{M2} = 65 \mu\text{M/s}$ ,  $K_2 = 1 \mu\text{M}$ ,  $V_{M3} = 500 \mu\text{M/s}$ ,  $K_A = 0.9 \mu\text{M}$ ,  $k = 10 \text{ s}^{-1}$ ,  $k_f = 1 \text{ s}^{-1}$ . Null-clines have been obtained by numerical resolution of  $dY/dt = 0$  and  $dZ/dt = 0$ , with  $dZ/dt$  and  $dY/dt$  given by eqs. (1).

spatially average values. Thus, to account for this kind of experiments, diffusion of cytosolic calcium (i.e. the last term of the first equation of system (1)) can be neglected. The temporal evolution of both cytosolic and intravesicular calcium at different levels of stimulation ( $\beta$ ) is shown in Fig. 2 (left panel). In the absence of stimulation, a stable steady state is established, corresponding to a low level of cytosolic calcium. Upon increasing the value of  $\beta$ , the steady state becomes unstable and sustained oscillations develop; in agreement with experimental results, the frequency of these oscillations increases with the level of CICR. In the present model, oscillations stop because the level of calcium in the calcium-sensitive pool (Y) becomes too low. However, as the calcium concentration in the pool is defined with respect to the total cell volume (which is, approximately, ten times larger than the volume of the intracellular stores), in the model, the level of Y never approaches zero. Recent experimental work has shown that, in hepatocytes, a cytosolic calcium spike corresponds to a decrease in the stores of less than half of its calcium level [42]. Another possibility for spike termination, put forward in other models [24,25], is that release stops because of the inhibition of the channel activity at levels of cytosolic calcium higher than the ones activating release [22,23]. Finally, when stimulation is too high (lower panel), oscillations stop and a high steady-state value of cytosolic calcium is established. This sequence of behaviours seen upon increasing stimulation is in agreement with observations in many cell types. Interestingly, in some cell types, physiological activity in response to calcium increases, has been shown to be lower for a constant high level of calcium than for an oscillatory calcium concentration in the cytosol [43].

One advantage of two-variable models is that one can follow their evolution in the phase space (Fig. 2, right panel). In such a representation, one plots the value of Y as a function of Z. The plane is divided in four distinct regions delimited by the two so-called "null-clines",  $dY/dt$  and  $dZ/dt=0$ . The intersection of these null-clines correspond to the steady-state. In the present model (eqs. (1)-(4a) or (4b)), one can show [44] that this steady-state is unstable if located on a region of sufficiently negative slope on the Z null-cline. Thus, in the upper panel, the steady state is stable. When stimulation is increased, the location of the steady-state enters a region of negative slope of the Z null-cline and thus becomes unstable. As the system is globally stable ( $dZ/dt$  and  $dY/dt$  tend to zero when Z and Y tend to infinity), the system can only quit this unstable steady-state to evolve towards a limit cycle corresponding to sustained oscillations. Finally, when stimulation becomes too high, the steady state is stable again, because the slope of the Z null-cline is then not sufficiently negative.

## 4. PROPAGATION OF TYPE 1 AND TYPE 2 CALCIUM WAVES

When taking cytosolic calcium diffusion into account in the one- or two-pool model based on CICR, one can easily obtain propagating calcium waves. Waves of type 1, i.e. fronts for which the wave length is smaller than the typical cell dimension, are illustrated in Fig. 3. Parameter values have been chosen to simulate the situation encountered in *Xenopus* oocytes [12,26,45] expressing receptors to acetylcholine. The latter transformation of the natural system has to be performed because these oocytes only exhibit one large, transient increase in cytosolic calcium upon fertilization, as most non-mammalian eggs. However, the properties of these artificially induced repetitive calcium waves have been extensively studied in that handy experimental system. In the conditions used in Fig. 3, numerical simulations show the propagation of waves characterized by a periodicity of 83 s and by

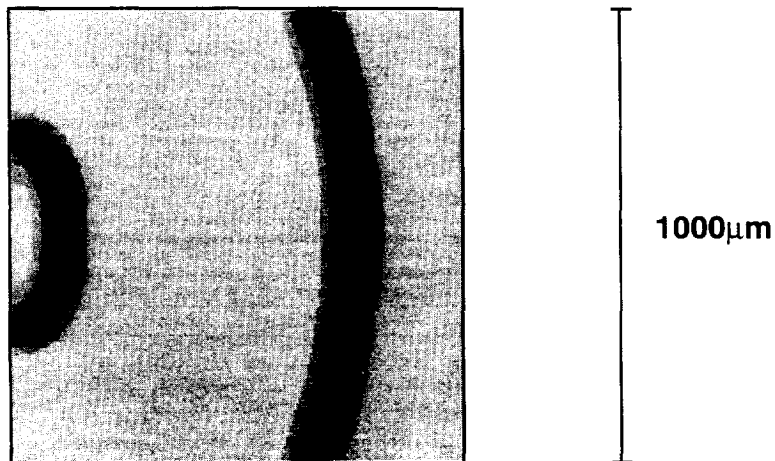


Fig.3. Modelling calcium waves of type 1 in *Xenopus* oocytes. The figure has been obtained by numerical simulations of the two-pool model based on CICR defined by eqs (1)-(4a) with  $v_0 = 3.1 \mu\text{M}/\text{min}$ ,  $K_R = 2 \mu\text{M}$ ,  $V_{M2} = 65 \mu\text{M}/\text{min}$ ,  $K_2 = 1 \mu\text{M}$ ,  $V_{M3} = 455 \mu\text{M}/\text{min}$ ,  $K_A = 0.9 \mu\text{M}$ ,  $k = 10 \text{ min}^{-1}$ ,  $k_f = 1 \text{ min}^{-1}$  and  $D_Z = 40 \mu\text{m}^2/\text{s}$ . The concentration of cytosolic calcium is represented by the grey level, with white corresponding to  $0 \mu\text{M}$  and black to  $1.5 \mu\text{M}$ . For simulating diffusion, the system is discretized into a grid of  $64 \times 64$  points. Constant stimulation ( $v_1\beta = 0.72 \mu\text{M}/\text{min}$ ) is applied in the central third part of the 2 first rows of points.

a propagation velocity equal to  $7.8 \mu\text{m}/\text{s}$ , in good agreement with experimental data [12,26,45]. In our simulations, these waves of type 1 correspond to successive fronts initiated by an oscillatory pacemaker located in the central left part of the system and propagating in an excitable medium.

In the model, both the period and the velocity decrease upon increasing the level of stimulation at the pacemaker site. In contrast, when increasing the excitability of the cytoplasm (by raising the rate of calcium entry from the extracellular medium,  $v_0$ ), the period decreases while the propagation

velocity increases. This latter theoretical result is in agreement with experimental observations [46]. On the other hand, the relationship between stimulation level and propagation velocity remains unclear and seems to differ from one cell type to another. A plausible explanation for this discrepancy could be that in some cell types, calcium stores are homogeneously distributed in the whole cytoplasm, while other cells possess discrete calcium stores separated by regions in which the calcium can only diffuse through nonexcitable cytoplasmic regions. In such cases, the distance between two successive stores determines the average velocity of calcium wave propagation [8,36].

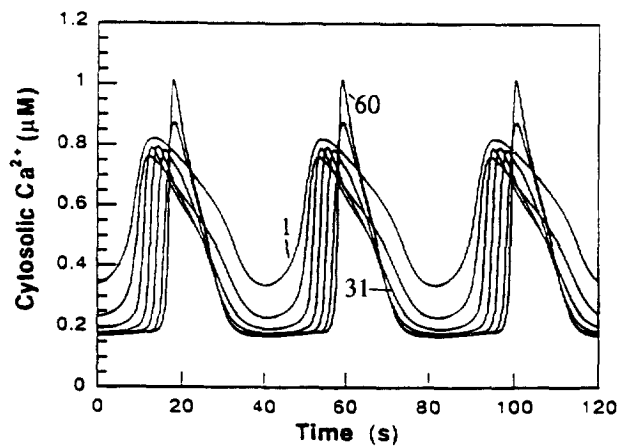


Fig.4. Modelling calcium waves of type 2 in hepatocytes. The figure has been obtained by numerical simulations of the two-pool model based on CICR defined by eqs (1)-(4a) with  $v_0 = 1.8 \mu\text{M}/\text{min}$ ,  $K_R = 2 \mu\text{M}$ ,  $V_{M2} = 93 \mu\text{M}/\text{min}$ ,  $K_2 = 1 \mu\text{M}$ ,  $V_{M3} = 500 \mu\text{M}/\text{min}$ ,  $K_A = 0.66 \mu\text{M}$ ,  $k = 5.6 \text{ min}^{-1}$ ,  $k_f = 1 \text{ min}^{-1}$  and  $D_Z = 400 \mu\text{m}^2/\text{s}$ . The level of cytosolic calcium is represented by the grey level, with white corresponding to  $0 \mu\text{M}$  and black to  $1.0 \mu\text{M}$ . For simulating diffusion, the system is discretized into a grid of  $60 \times 60$  points. Constant stimulation ( $v_1\beta = 22.8 \mu\text{M}/\text{min}$ ) is applied in the central third part of the 2 first rows of points. The curves represent the time evolution of cytosolic calcium concentration in the middle of columns 1, 11, 21, 31, 51 and 60 of the spatial grid.

In most cell types, the calcium increase in response to stimulation invades the whole cell, before declining homogeneously back to the basal level. These type-2 waves can also be obtained in the model, when one considers smaller cells or/and cells in which the kinetics of calcium exchange between the stores and the cytosol is rather slow, in comparison with type-1 waves. Such a system is shown in Fig. 4, aimed to simulate the situation encountered in hepatocytes, whose length is here supposed to be 4 times smaller than in oocytes. In contrast with Fig. 3 in which successive "pictures" of the system are shown, Fig. 4 shows the temporal evolution of the calcium level at increasing distances from the stimulation level. It is clearly visible that the



return of the calcium concentration to the basal level occurs more or less uniformly in the whole system, in agreement with experimental observations on hepatocytes [10]. The period and velocity of the calcium waves are equal to 41s and  $53 \mu\text{m/s}$ , respectively. Interestingly, the best qualitative agreement with experimental observations performed on type-2 waves is obtained when all parts of the system are spontaneously oscillating, i.e. for phase waves. That some cell types may in certain conditions display calcium phase waves has also been suggested by another theoretical study [47].

##### 5. SIMULATION OF SPIRAL CALCIUM WAVES AS OBSERVED IN CARDIAC MYOCYTES

In numerical simulations, spiral waves are generally created by somewhat artificial ways, i.e. by an appropriate choice of initial conditions, or through

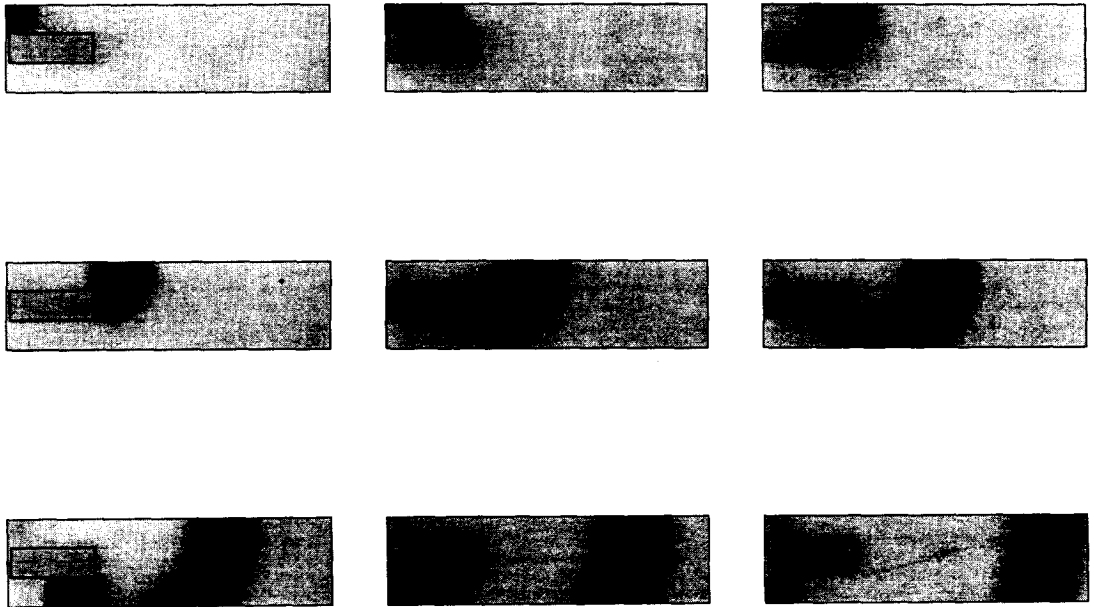


Fig.5. Spiral calcium wave propagation around a region impermeable to calcium diffusion, in a system whose geometry resembles that of a myocyte. The cell is supposed to be  $100 \times 27 \mu\text{m}$ , and the obstacle  $25.5 \times 9 \mu\text{m}$ . The system is discretized into  $200 \times 60$  grid points for numerical integration. The distance between the left part of the plasma membrane and the obstacle is  $4 \mu\text{m}$  and, vertically, it is just in the middle. Stimulation ( $v_1\beta$ ) is applied in the top left corner. The figure has been obtained by numerical simulations of the two-pool model based on CICR defined by eqs (1)-(4a) with  $v_0 = 3.3 \mu\text{M/s}$ ,  $v_1 = 2.3 \mu\text{M/s}$ ,  $K_R = 2 \mu\text{M}$ ,  $V_{M2} = 80 \mu\text{M/s}$ ,  $K_2 = 1 \mu\text{M}$ ,  $V_{M3} = 455 \mu\text{M/s}$ ,  $K_A = 0.93 \mu\text{M}$ ,  $k = 10 \text{ s}^{-1}$ ,  $k_f = 1 \text{ s}^{-1}$  and  $D_Z = 225 \mu\text{m}^2/\text{s}$ . The level of cytosolic calcium is represented by the grey level, with white corresponding to  $0 \mu\text{M}$  and black to  $1.5 \mu\text{M}$ . Time is increasing from left to right and from top to bottom; time interval between two successive panels is 80 ms. Sustained wave propagation is characterized by a period of 80 ms and a mean velocity of  $132 \mu\text{m/s}$ .

breaking concentric waves by making some region of the system transiently refractory. These mechanisms have been used to simulate spiral calcium waves resembling those observed in *Xenopus* oocytes [24,25,45,47].

Following careful observation of waves propagating in calcium-overloaded myocytes, Lipp and Niggli [13] have suggested that, when spirals are initiated, they result from the collision of a planar front on a cell nucleus. Initial theoretical results have shown that calcium fronts of type 1 can be obtained on the basis of the CICR mechanism when considering a thin, elongated cell resembling a cardiac myocyte. When choosing parameter values such as to get periods of the order of a few seconds, these waves naturally appear as type 1 waves propagating with velocities of the order of 100  $\mu\text{m/s}$  [8]. Using the same CICR model, we have recently shown that, in appropriate circumstances, a spiral wave can be initiated, regardless of initial conditions, when a calcium front of type-1 encounters a region lacking calcium pools [48]. Alternatively, a barrier to diffusion may also suffice to initiate the spiral wave (see Fig. 5). From an experimental point of view, whether cytosolic calcium can diffuse inside the nucleus of the myocyte remains an unresolved question. Numerical simulations indicate, however, that, for spirals to occur, the obstacle must be well-placed with respect to the pacemaker region. This might explain why planar waves are much more commonly observed than spirals [13,14].

## 6. CONCLUSION

Calcium signalling provides an excellent prototype of temporally and spatially auto-organized system at the cellular level. Most properties of oscillations and waves can be qualitatively understood by resorting to a simple autocatalytic mechanism, whereby calcium activates its own release from intracellular stores. Much work however remains to be done to clarify the physiological significance of such a highly developed mode of intracellular signalling.

### *Acknowledgements*

*This work was supported by the programme "Actions de Recherche Concertée" (ARC 94-99/180) launched by the Division of Scientific Research, Ministry of Science and Education, French Community of Belgium and by grant 3.4588.93 from the Fonds de la Recherche Scientifique Médicale.*

## REFERENCES

1. BERRIDGE M.J., Inositol trisphosphate and calcium signalling. *Nature* **361**, 315-325 (1993).
2. BERRIDGE M.J. & DUPONT G., Spatial and temporal signalling by calcium. *Curr. Opin. Cell Biol.* **6**, 267-274 (1994).
3. GOLDBETER A., *Biochemical Oscillations and Cellular Rhythms. The Molecular bases of periodic and chaotic behaviour.* Cambridge University Press (1996).
4. DUPONT G. & GOLDBETER, A., Protein phosphorylation driven by intracellular calcium oscillations: a kinetic analysis. *Biophys.Chem.* **42**, 257-270 (1992).

4. DUPONT G. & GOLDBETER, A., Protein phosphorylation driven by intracellular calcium oscillations: a kinetic analysis. *Biophys.Chem.* **42**, 257-270 (1992).
5. MEYER T. & STRYER L., Calcium spiking. *Annu. Rev. Biophysics Biophys. Chem.* **20**, 153-174 (1991).
6. JAFFE, L.F., The path of calcium in cytosolic calcium oscillations: a unifying hypothesis. *Proc. Natl. Acad. Sci. USA* **88**, 9883-9887 (1991).
7. TAKAMATSU T. & WIER W., Calcium waves in mammalian heart: quantification of origin, magnitude, waveform and velocity. *FASEB J.* **4**, 1519-1525 (1990).
8. DUPONT G. & GOLDBETER A., Oscillations and waves of cytosolic calcium: insights from theoretical models. *BioEssays* **14**, 485-493 (1992).
9. TSIEN R.W. & TSIEN R.Y., Calcium channels, stores and oscillations. *Annu. Rev. Cell Biol.* **6**, 715-760 (1990).
10. THOMAS A.P., RENARD D.C. & ROONEY T.A., Spatial and temporal organization of calcium signalling in hepatocytes. *Cell Calcium* **12**, 111-116 (1991).
11. JACOB R., Calcium oscillations in electrically non-excitabile cells. *Biochim. Biophys. Acta* **1052**: 427-438 (1990).
12. LECHLEITER J., GIRARD S., PERALTA E. & CLAPHAM D., Spiral calcium wave propagation and annihilation in *Xenopus laevis* oocytes. *Science* **252**, 123-126 (1991).
13. LIPP P. & NIGGLI E., Microscopic spiral waves reveal positive feedback in subcellular calcium signaling. *Biophys. J.* **65**, 2272-2276 (1993).
14. ENGEL J., FECHNER M., SOWERBY A., FINCH S. & STIER A., Anisotropic propagation of Ca<sup>2+</sup> waves in isolated cardiomyocytes. *Biophys. J.* **66**, 1756-1762 (1994).
15. NICOLIS G. & PRIGOGINE I., *Self-organization in Nonequilibrium systems. From Dissipative Structures to Order through Fluctuations*. Wiley, New-York.
16. MEYER T. AND STRYER L., Molecular model for receptor-stimulated calcium spiking. *Proc. Natl. Acad. Sci. USA* **85**, 5051-5055 (1988).
17. CUTHBERTSON, K. & CHAY T., Modelling receptor-controlled intracellular calcium oscillations *Cell Calcium* **12**, 111-116 (1991).
18. FABIATO A. & FABIATO F., Contractions induced by a calcium-triggered release of calcium from the sarcoplasmic reticulum of single skinned cardiac cells. *J. Physiol.* **249**, 469-495 (1975).
19. KUBA K. & TAKESHITA. S., Simulation of intracellular calcium oscillations in a sympathetic neurone. *J. Theor. Biol.* **93**: 1009-1031 (1981).
20. GOLDBETER A., DUPONT G. & BERRIDGE M. Minimal model for calcium oscillations and for their frequency encoding through protein phosphorylation. *Proc. Natl. Acad. Sci. USA* **87**, 1461-1465 (1990).
21. DUPONT G., BERRIDGE M.J. & GOLDBETER A., Signal-induced Ca<sup>2+</sup> oscillations: properties of a model based on Ca<sup>2+</sup>-induced Ca<sup>2+</sup> release. *Cell Calcium* **12**, 73-86 (1991).
22. FINCH E., TURNER T. & GOLDEN S., Calcium as coagonist of inositol 1,4,5-trisphosphate-induced calcium release. *Science* **252**, 443-446 (1991).
23. BEZPROZVANNY I. & EHRLICH B., Inositol (1,4,5)-trisphosphate (InsP<sub>3</sub>)-gated Ca channels from cerebellum: conduction properties for divalent cations and regulation by intraluminal calcium. *J. Gen. Physiol.* **104**, 821-856 (1994).
24. SNEYD J., KEIZER J. & SANDERSON M.J., Mechanisms of calcium oscillations and waves: a quantitative analysis. *FASEB J.* **9**, 1463-1472 (1995).
25. TANG Y., STEPHENSON J. & OTHMER H.G., Simplification and analysis of models of calcium dynamics based on IP<sub>3</sub>-sensitive calcium channel kinetics. *Biophys. J.* **70**, 246-263 (1996).
26. LECHLEITER J. & CLAPHAM D., Molecular mechanism of intracellular calcium excitability in *X. Laevis*. *Cell* **69**, 283-294 (1992).
27. DELISLE S. & WELSH M., Inositol trisphosphate is required for the propagation of calcium waves in *Xenopus* oocytes. *J. Biol. Chem.* **267**, 7963-7966 (1992).
28. MELDOLESI J., MADEDDU L. & POZZAN T., Intracellular storage organelles in non-muscle cells: heterogeneity and functional assignment. *Biochim. Biophys. Acta* **1055**: 134-140 (1990).

29. LAW G., PACHTER A., THASTRUP O., HANLEY R. & DANNIES P., Thapsigargin, but not caffeine, blocks the ability of thyrotropin-releasing hormone to release  $\text{Ca}^{2+}$  from an intracellular store in GH4C1 pituitary cells. *Biochem. J.* **267**, 359-364 (1990).
30. WALTON P., AIREY J., SUTKO J., BECK C., MIGNERY G., SUDHOF T., DEERINCK T. & ELLISMAN M., Ryanodine and inositol trisphosphate receptors coexist in avian cerebellar Purkinje neurons. *J. Cell Biol.* **113**, 1145-1157 (1991).
31. GROMADA J., JORGENSEN T. & DISSING S., Cyclic ADP-ribose and inositol 1,4,5-trisphosphate mobilizes  $\text{Ca}^{2+}$  from distinct intracellular pools in permeabilized lacrimal acinar cells. *FEBS Lett.* **360**, 303-306 (1995).
32. BLATTER L. & WIER G., Agonist-induced  $[\text{Ca}^{2+}]_i$  waves and  $\text{Ca}^{2+}$ -induced  $\text{Ca}^{2+}$  release in mammalian vascular smooth muscle cells. *Am. J. Physiol.* **263**, H576-H586 (1992).
33. GALIONE A., MCDUGALL A., BUSA W., WILLMOTT N., GILLOT I. & WHITAKER M., Redundant mechanisms of calcium-induced calcium release underlying calcium waves during fertilization of sea urchin eggs. *Science* **261**, 348-352 (1993).
34. BERRIDGE M.J., A tale of 2 messengers, *Nature* **365**, 388-389 (1993).
35. ALLEN G., MUIR S. & SANDERS D., Release of  $\text{Ca}^{2+}$  from individual plant vacuoles by both  $\text{IP}_3$  and cyclic ADP-ribose, *Science* **268**, 735-737 (1995).
36. DUPONT G. & GOLDBETER A., Properties of intracellular  $\text{Ca}^{2+}$  waves generated by a model based on  $\text{Ca}^{2+}$ -induced  $\text{Ca}^{2+}$  release. *Biophys. J.* **67**, 2191-2204 (1994).
37. DUPONT G. & GOLDBETER A., One-pool model for  $\text{Ca}^{2+}$  oscillations involving  $\text{Ca}^{2+}$  and inositol 1,4,5-trisphosphate as co-agonists for  $\text{Ca}^{2+}$  release. *Cell Calcium* **14**, 311-322 (1993).
38. BERRIDGE M.J., Capacitative calcium entry, *Biochem. J.* **312**, 1-11 (1995).
39. THORN P.,  $\text{Ca}^{2+}$  influx during agonist and  $\text{Ins}(2,4,5)\text{P}_3$ -evoked  $\text{Ca}^{2+}$  oscillations in HeLa epithelial cells, *J. Physiol.* **482**, 275-281 (1995).
40. BODE H. & NETTER K., Agonist-releasable intracellular calcium stores and the phenomenon of store-dependent  $\text{Ca}^{2+}$  entry. *Biochem. Pharmacol.* **51**, 993-1001 (1996).
41. DUPONT G., BERRIDGE M.J. & GOLDBETER A., Latency correlates with period in a model for signal-induced  $\text{Ca}^{2+}$  oscillations based on  $\text{Ca}^{2+}$ -induced  $\text{Ca}^{2+}$  release. *Cell Regul.* **1**, 853-861 (1990).
42. CHATTON J., LIU H. & STUCKI J., Simultaneous measurements of  $\text{Ca}^{2+}$  in the intracellular stores and the cytosol of hepatocytes during hormone-induced  $\text{Ca}^{2+}$  oscillations. *FEBS Lett.* **368**, 165-168 (1995).
43. LAW G., PACHTER A. & DANNIES P., Ability of repetitive  $\text{Ca}^{2+}$  spikes to stimulate prolactin release is frequency dependent. *Biophys. Res. Commun.* **158**, 811-816 (1989).
44. GOLDBETER A. & DUPONT G., Allosteric regulation, cooperativity, and biochemical oscillations. *Biophys. Chem.* **37**, 341-353 (1990).
45. GIRARD S., LUCKHOFF A., LECHLEITER J., SNEYD J. & CLAPHAM D., Two-dimensional model of calcium waves reproduces the patterns observed in *Xenopus* oocytes. *Biophys. J.* **61**, 509-517 (1992).
46. GIRARD S. & CLAPHAM D., Acceleration of intracellular calcium waves in *Xenopus* oocytes by calcium influx. *Science* **260**, 229-232 (1993).
47. JAFRI M. & KEIZER J., On the roles of calcium diffusion, calcium buffers, and the endoplasmic reticulum in  $\text{IP}_3$ -induced  $\text{Ca}^{2+}$  waves. *Biophys. J.* **69**, 2139-2153 (1995).
48. DUPONT G., PONTES J. & GOLDBETER A., Modeling spiral  $\text{Ca}^{2+}$  waves in single cardiac cells: role of the spatial heterogeneity created by the nucleus. *Am. J. Physiol.*, in press (1996).